A Mathematical Model of Bone Remodeling Process: Effects of Parathyroid Hormone and Vitamin D

Chontita Rattanakul, Sahattaya Rattanamongkonkul, Wannapa Kunpasuruang,

Sittipong Ruktamatakul and Saowaros Srisuk

***Abstract*—**Parathyroid hormone and vitamin D play an important role in calcium homeostasis as well as in bone remodeling process. We propose here a system of nonlinear differential equations to describe bone remodeling process accounted for the concentrations of parathyroid hormone and vitamin D, the number of active osteoclasts and the number of active osteoblasts. We then utilize the singular perturbation technique to analyze our model in order to obtain the delineating conditions on the system parameters for which the different kinds of dynamic behavior can be occurred. The model is then investigated numerically. The theoretical and numerical results show that a periodic behavior which corresponds to the pulsatile pattern observed clinically in the levels of parathyroid hormone and vitamin D can be expected from our model.

***Keywords*—**bone remodeling, mathematical model, parathyroid hormone, singular perturbation, vitamin D.

Manuscript received August 8, 2011. This work was supported by the Centre of Excellence in Mathematics, Commission on Higher Education, Thailand and the Faculty of Science, Mahidol University, Thailand.

C. Rattanakul is with the Department of Mathematics, Faculty of Sciences, Mahidol University, Thailand and the Centre of Excellence in Mathematics, the Commission on Higher Education, Thailand (corresponding author, phone: 662-201-5340; fax: 662-201-5343; e-mail: sccrt@mahidol.ac.th).

S. Rattanamongkonkul is with the Department of Mathematics, Faculty of Sciences, Burapha University, Thailand and the Centre of Excellence in Mathematics, the Commission on Higher Education, Thailand (e-mail: sahattay@buu.ac.th).

W. Kunpasuruang is with the Department of Mathematics, Faculty of Science, Silpakorn University, Thailand and the Centre of Excellence in Mathematics, the Commission on Higher Education, Thailand (e-mail: wannapa@su.ac.th).

S. Ruktamatakul is with the Department of Mathematics, Faculty of Liberal Arts Science, Kasetsart University, Thailand and the Centre of Excellence in Mathematics, the Commission on Higher Education, Thailand (e-mail: faasspr@nontri.ku.ac.th).

S. Srisuk is with the Department of Mathematics, Faculty of Sciences, Burapha University, Thailand and the Centre of Excellence in Mathematics, the Commission on Higher Education, Thailand (e-mail: saowaros.srisuk@gmail.com).

I. Introduction

SUITABLE amounts of calcium in its ionized form are needed for normal function of all cells [1]. Calcium ion controls a wide range of biological processes and is one of the principal components of bone. In human, maintenance of suitable concentrations calcium ion in the extracellular fluid requires the activity of two hormones, parathyroid hormone (PTH) and a derivative of vitamin D called calcitriol [1]. PTH promotes the transfer of calcium from bone into the extracellular fluid. It acts on bone cells to promote calcium mobilization through bone remodeling process and on renal tubules to promote reabsorbtion calcium and excretion of phosphate [1]. The rate of PTH secretion is inversely related to the concentration of blood calcium, which directly inhibits secretion by the chief cells of the parathyroid glands [1]. Vitamin D metabolite also promotes calcium mobilization from bone and reinforces the actions of PTH on this process. Bone remodeling process can be viewed as step by step as follows. At first, bone resorbing cells called osteoclasts appear on the surface of bone remodeling unit and excavate a lacuna on the surface of bone. Osteoclasts are then replaced by bone forming cells called osteoblasts. Osteoblasts then refill the resorption cavity and become osteocytes, the inactive form of osteoblasts [2], [3]. Many factors involve in bone remodeling process including PTH, vitamin D, calcitonin, and estrogen.

Many mathematical models have been proposed to describe bone remodeling process. However, PTH and vitamin D have not been incorporate in the model together. Therefore, in this paper, we will focus on the effects of PTH and vitamin D on the number of active osteoclasts and the number of active osteoblasts in bone remodeling process [1]-[3].

II. Model Development

We now propose a system of nonlinear differential equations to describe bone remodeling process based on the effects of PTH and vitamin D as follows. Let us denote the concentration of PTH above the basal level at time t by $X(t)$, the serum level of vitamin D at time t by $Y(t)$, the number of active osteoclasts at time t by $Z(t)$, and the number of active osteoblasts at time t

by $W(t)$. At first, we assume that the high levels of osteoclast and osteoblast precursors lead to the high levels of active osteoclastic and osteoblastic cells, respectively, which result from the differentiation, and activation of their precursors.

PTH is produced from the parathyroid gland. The secretion of PTH is principally controlled by the concentration of calcium ion in extracellular fluid [4]. Since the more active osteoclasts mean the more calcium release from bone, therefore the level of serum calcium varies directly with the number of active osteoclasts. When the calcium concentration increases, the secretion of PTH decreases [5]. Thus, the level of serum calcium varies inversely with the secretion of PTH. However, low levels of PTH are secreted even when blood calcium levels are high [4]. On the other hand, vitamin D has a negative feedback on PTH secretion, thus the increase in the level of vitamin D results in the decrease in the level of PTH [1]. The equation for the rate of PTH secretion above the basal level is then assumed to take the form

$$\frac{dX}{dt} = \frac{a_1}{(k_1 + Y)(k_2 + Z)} - b_1 X \tag{1}$$

where a_1, b_1, k_1 and k_2 are positive constants.

Vitamin D plays an important role in maintaining the level of calcium in blood within the normal rage by enhancing the efficiency of intestinal calcium absorption and by increasing the mobilization of stem cells to become osteoclasts that, in turn, mobilize calcium stores from bone [5]-[8]. In addition, the increase in the level of PTH results in the increase in the synthesis of calcitriol, the active form of vitamin D [1], [9]. Therefore, the equation for the rate of change in serum level of vitamin D is then assumed to have the form

$$\frac{dY}{dt} = \frac{a_2 + a_3 X}{k_3 + Z} - b_2 Y \tag{2}$$

where a_2, a_3, k_3 and b_2 are positive constants.

Osteoclasts are responsible for bone resorption deriving from hemopoietic stem cells of the monocyte/macrophage lineage [10]. Although the dominant activators of bone resorption and osteoclast activation are PTH and vitamin D, osteoclasts do not possess receptors for either PTH or vitamin D [11]. Thus, the activation process involving PTH and vitamin D is believed to occur as a consequence of PTH/vitamin D interacting with its receptors on osteoblasts. Then, the active osteoblasts release paracrine agents which then achieve activation of osteoclasts, so that the bone-resorptive event is initiated [11]. Therefore, the dynamics of the active osteoclastic population can be described by the following equation

$$\frac{dZ}{dt} = \left(\frac{a_4 + a_5 X}{k_4 + X^2} \right) YZW - b_3 Z \tag{3}$$

where a_4, a_5, b_3 and k_4 are positive constants.

Osteoblasts are responsible for bone formation originated from the mesenchymal stem cells. Many factors involve in the proliferation and differentiation of osteoblasts including FGF, IGF-I, TGF-beta [12]. On the other hand, the effect of PTH on the proliferation and differentiation of osteoblasts are both stimulating and inhibiting [13]. In addition, vitamin D has been found to stimulate the proliferation and differentiation of active osteoblastic cells [14]. The dynamics of the osteoblastic population can be described by the following equation

$$\frac{dW}{dt} = \left(\frac{a_6 - a_7 W}{k_5 + X} \right) X + \frac{a_8 YW}{k_6 + Y} - b_4 W \tag{4}$$

where a_6, a_7, a_8, b_4, k_5 and k_6 are positive constants.

III. SINGULAR PERTURBATION ANALYSIS

In what follows, we assume that PTH has the very fast dynamics, Vitamin D has the fast dynamics. The osteoclastic population possesses the slow dynamics and the osteoblastic population has the slowest dynamics. Consequently, we scale the dynamics of the three components and parameters of the system in term of small positive parameters $0 < \varepsilon < 1$, $0 < \delta < 1$ and $0 < \eta < 1$ as follows.

Letting $x = X, y = Y, z = Z, w = W, c_1 = a_1, c_2 = \frac{a_2}{\varepsilon}, c_3 = \frac{a_3}{\varepsilon}$, $c_4 = \frac{a_4}{\varepsilon\delta}, c_5 = \frac{a_5}{\varepsilon\delta}, d_1 = b_1, d_2 = \frac{b_2}{\varepsilon}, d_3 = \frac{b_3}{\varepsilon\delta}$, we are led to the following model equations:

$$\frac{dx}{dt} = \frac{c_1}{(k_1 + y)(k_2 + z)} - d_1 x \equiv f(x, y, z, w) \tag{5}$$

$$\frac{dy}{dt} = \varepsilon \left(\frac{c_2 + c_3 x}{k_3 + z} - d_2 y \right) \equiv \varepsilon g(x, y, z, w) \tag{6}$$

$$\frac{dz}{dt} = \varepsilon\delta \left(\left(\frac{c_4 + c_5 x}{k_4 + x^2} \right) yzw - d_3 z \right) \equiv \varepsilon\delta h(x, y, z, w) \tag{7}$$

$$\frac{dw}{dt} = \varepsilon\delta\eta \left(\left(\frac{c_6 - c_7 w}{k_5 + x} \right) x + \frac{c_8 yw}{k_6 + y} - d_4 w \right) \equiv \varepsilon\delta\eta k(x, y, z, w) \tag{8}$$

The shapes and relative positions of the manifolds $\{f = 0\}, \{g = 0\}$, $\{h = 0\}$ and $\{k = 0\}$ determine the shapes, directions and speeds of the solution trajectories. We now analyze each of the equilibrium manifolds in details.

The manifold $\{f = 0\}$

This manifold is given by the equation

$$x = \frac{c_1}{d_1 (k_1 + y)(k_2 + z)} \equiv A(y, z) \tag{9}$$

which is a decreasing function of *y* and *z*. It intersects the *x*-axis on the (x, y) – plane at the point where

$$x = \frac{c_1}{d_1 k_1 k_2} \equiv x_1 \tag{10}$$

The manifold $\{g=0\}$

This manifold is given by the equation

$$y=\frac{1}{d_2}\left(\frac{c_2+c_3x}{k_3+z}\right)\equiv B(x,z) \tag{11}$$

which is an increasing function of *y* and a decreasing function of *z*. It intersects the *y*-axis on the $(x,y)-$plane at the point where

$$y=\frac{c_2}{d_2k_3}\equiv y_1 \tag{12}$$

Moreover, the manifold $\{f=0\}$ intersects the manifold $\{g=0\}$ along the curve

$$x=\frac{c_1}{d_1\left(k_1+B(x,z)\right)\left(k_2+z\right)} \tag{13}$$

which intersects the $(x,y)-$plane at the point where $z=0$

$$x=\frac{\left\{\begin{array}{l}-d_1k_2\left(d_2k_1k_3+c_2\right)+\\ \sqrt{\left[d_1k_2\left(d_2k_1k_3+c_2\right)\right]^2+4c_1c_3d_1d_2k_2k_3}\end{array}\right\}}{2c_3d_1k_2}\equiv x_2 \tag{14}$$

and

$$y=\frac{c_2+c_3x_3}{d_2k_3}\equiv y_2 \tag{15}$$

The manifold $\{h=0\}$

This manifold consists of two submanifold which are the trivial manifold $z=0$ and the nontrivial manifold

$$y=\frac{d_3}{w}\left(\frac{k_4+x^2}{c_4+c_5x}\right)\equiv C(x,w) \tag{16}$$

The nontrivial manifold is independent of the variable *z* and thus this submanifold is parallel to the *z*-axis. It attains the relative minimum at the point where

$$x=\frac{-c_4\pm\sqrt{c_4^2+c_5^2k_4}}{c_5}\equiv x_m \tag{17}$$

and

$$y=\frac{d_3}{w}\left(\frac{k_4+x_m^2}{c_4+c_5x_m}\right)\equiv y_m(w) \tag{18}$$

On the other hand, the nontrivial manifold intersects the *y*-axis on the (*x*,*y*)-plane at the point where

$$y=\frac{d_3k_4}{c_4w}\equiv y_3(w) \tag{19}$$

Moreover, the manifold $\{f=0\}$ intersects the nontrivial manifold $\{h=0\}$ along the curve

$$x=\frac{c_1}{d_1\left(k_1+C(x,w)\right)\left(k_2+z\right)} \tag{20}$$

which has a relative minimum point $L\left(x_m,y_m(w),z_m(w)\right)$ where

$$z_m(w)=\frac{c_1}{d_1\left(k_1+y_m\right)x_m}-k_2 \tag{21}$$

Also, the curve $\{f=h=0\}$ intersects the (*x*,*y*)-plane at the point where $z=0$, $x=x_3(w)$, $x_3(w)$ is a root of

$$\begin{array}{l}\left(d_1d_3k_2\right)x^3+\left(c_5d_1k_1k_2w\right)x^2\\ +\left(d_1k_2\left(c_4k_1w+d_3k_4\right)-c_1c_5w\right)x-c_1c_4w=0\end{array} \tag{22}$$

and

$$y=\frac{d_3}{w}\left(\frac{k_4+x_2^2(w)}{c_4+c_5x_2(w)}\right)\equiv y_4(w) \tag{23}$$

Note that $x_3(w)$ is only one positive root of (19) if

$$d_1k_2\left(c_4k_1w+d_3k_4\right)<c_1c_5w \tag{24}$$

The manifold $\{k=0\}$

This manifold is given by the equation

$$w=\frac{c_6x\left(k_6+y\right)}{c_7x\left(k_6+y\right)-c_8y\left(k_5+x\right)+d_4\left(k_5+x\right)\left(k_6+y\right)}\equiv D(x,y) \tag{25}$$

which is independent of the variable *z*.

Case I: If ε and δ are sufficiently small and the inequality (24) holds and the inequalities

$$x_m<x_S<x_2<x_3(w) \tag{26}$$

and

$$y_4(w)<y_2<y_3(w) \tag{27}$$

are satisfied where all the parametric values are given as above, then the manifolds are positioned as in Fig. 1 and the system of (5)-(8) will have a periodic solution. Here, the transitions of slow, intermediate and high speeds are indicated by one, two and three arrows, respectively.

In Fig. 1, without loss of generality, we start from point *I* and we assume that the position of *I* is as in Fig. 1 with $\{f\neq 0\}$. A very fast transition will bring the solution trajectory to point *J* on the manifold $\{f=0\}$. Here, $\{g<0\}$ and a transition at fast speed will be made in the direction of decreasing *y* until point *K* on the curve $\{f=h=0\}$ is reached. A fast transition then follows along this curve to some point *L* where the stability of submanifold will be lost. A jump to point *M* on the other stable part of $\{f=h=0\}$ followed by a fast transition in the direction of increasing *y* until the point *N* is reached since $\{g>0\}$ here. Once the point *N* is reached the stability of submanifold will be lost. A jump to point *O* on the other stable part of $\{f=h=0\}$ followed by a fast transition in the direction of decreasing *y* since $\{g<0\}$ here.

Consequently, a fast transition will bring the system back to the point *L*, followed by flows along the same path repeatedly, resulting in the closed orbit *LMNOL*. Thus, limit cycle in the system for ε, δ and η are sufficiently small exists.

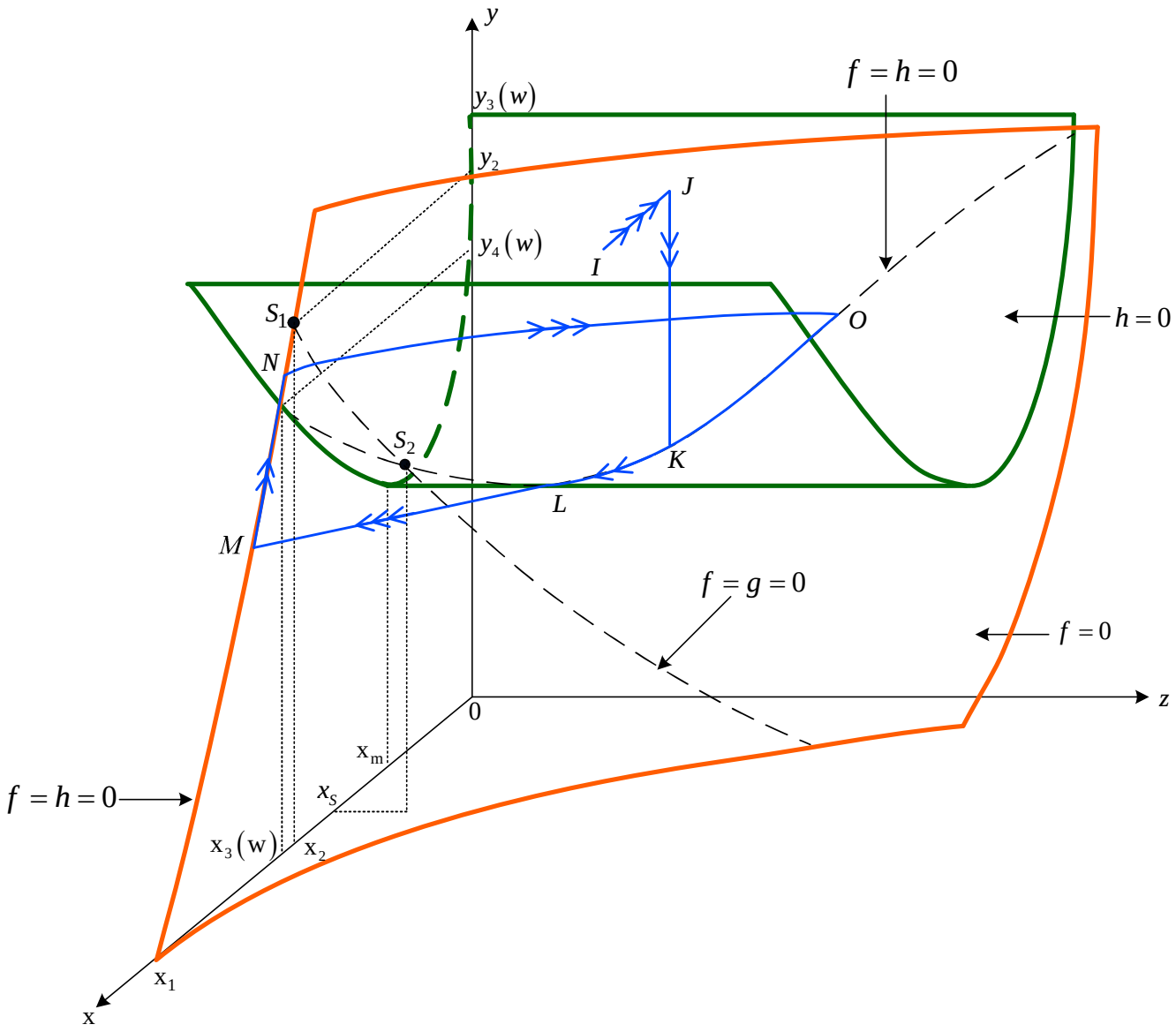

Fig. 1 The three equilibrium manifolds $\{f = 0\}, \{g = 0\}$ and $\{h = 0\}$ in the (x, y, z) – space in Case 1. Segments of the trajectories with one, two, and three arrows represent slow, fast, and very fast transitions, respectively.

Case II: If ε and δ are sufficiently small and the inequality (24) holds and the inequalities

$$x_m < x_3(w) < x_2 \tag{28}$$

and

$$y_2 < y_4(w) < y_3(w) \tag{29}$$

are satisfied where all the parametric values are given as above, then the manifolds are positioned as in Fig. 2 and the system of (5)-(8) will have a stable equilibrium point.

In Fig. 2, without loss of generality, we start from point I and we assume that the position of I is as in Fig. 2 with $\{f \neq 0\}$. A very fast transition will bring the solution trajectory to point J on the manifold $\{f = 0\}$. Here, $\{g < 0\}$ and a transition at fast speed will be made in the direction of decreasing y until point K on the curve $\{f = g = 0\}$ is reached followed by a slow transition in the direction of decreasing z until the steady state S_1 where $f = g = h = 0$ is reached since $\{h < 0\}$ here. Thus, the solution trajectory is expected in this case to tend toward this stable equilibrium point S_1 as time passes.

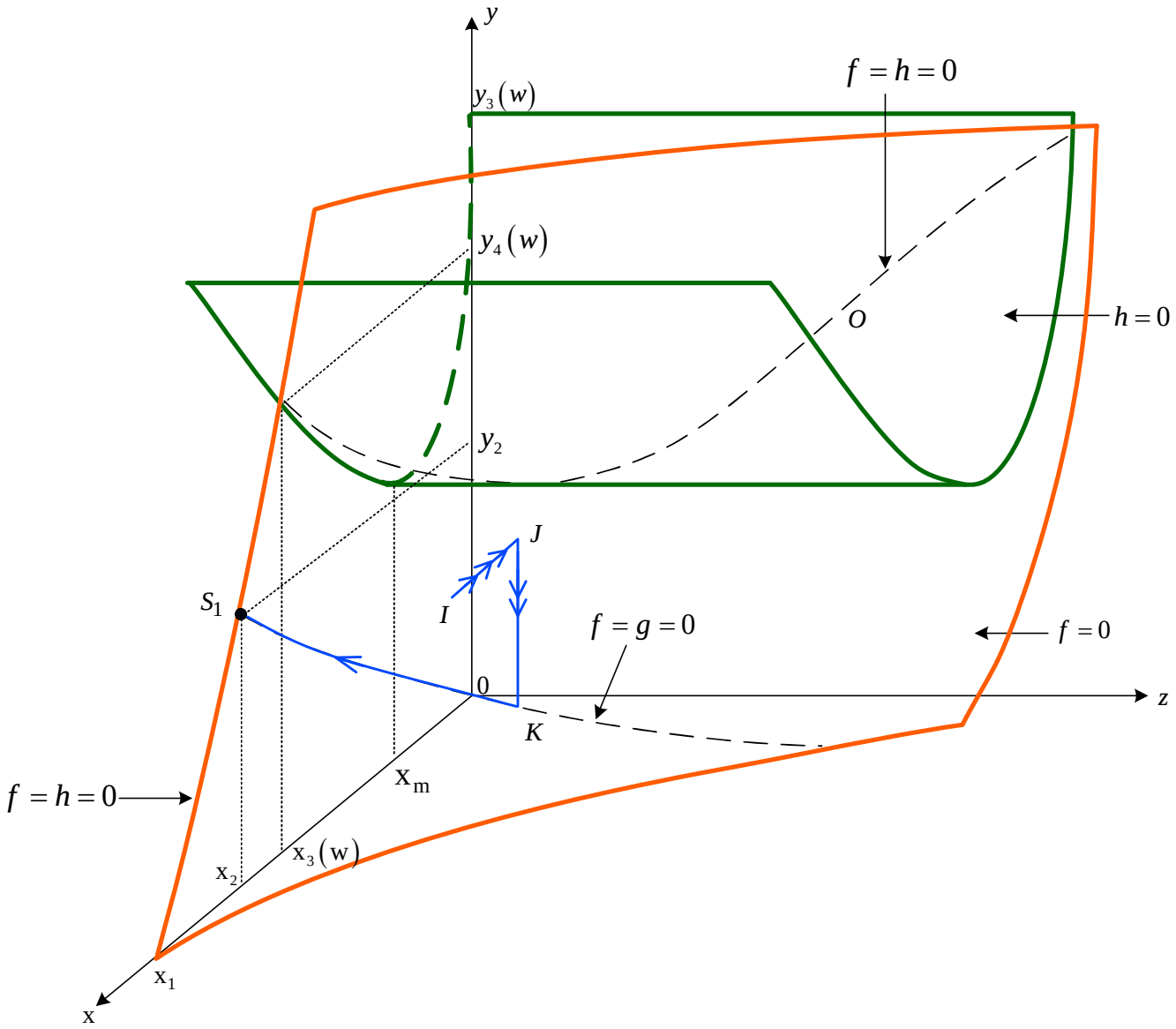

Fig. 2 The three equilibrium manifolds $\{f = 0\}, \{g = 0\}$ and $\{h = 0\}$ in the (x, y, z) – space in Case 2. Segments of the trajectories with one, two, and three arrows represent slow, fast, and very fast transitions, respectively.

Case III: If ε and δ are sufficiently small and the inequality (24) holds and the inequalities

$$x_S < x_m < x_2 < x_3(w) \tag{30}$$

and

$$y_4(w) < y_2 < y_3(w) \tag{31}$$

are satisfied where all the parametric values are given as above, then the manifolds are positioned as in Fig. 3 and the system of (4)-(6) will have a stable equilibrium point.

In Fig. 3, without loss of generality, we start from point I and we assume that the position of I is as in Fig. 3 with $\{f \neq 0\}$. A very fast transition will bring the solution trajectory to point J on the manifold $\{f = 0\}$. Here, $\{g < 0\}$ and a transition at fast speed will be made in the direction of decreasing y until point K on the curve $\{f = h = 0\}$ is reached followed by a fast transition in the direction of decreasing y to the point L where the stability of submanifold will be lost. A jump to point M on the other stable part of $\{f = h = 0\}$ followed by a fast transition in the direction of increasing y until the point N is reached since $\{g > 0\}$ here. Once the point N is reached the stability of submanifold will be lost. A jump to point O on the other stable part of $\{f = h = 0\}$ followed by a fast transition in the direction of decreasing y, since $\{g < 0\}$ here, until the steady state S_2 where $f = g = h = 0$ is reached. Thus, the solution trajectory is expected in this case to tend toward this stable equilibrium point S_2 as time passes.

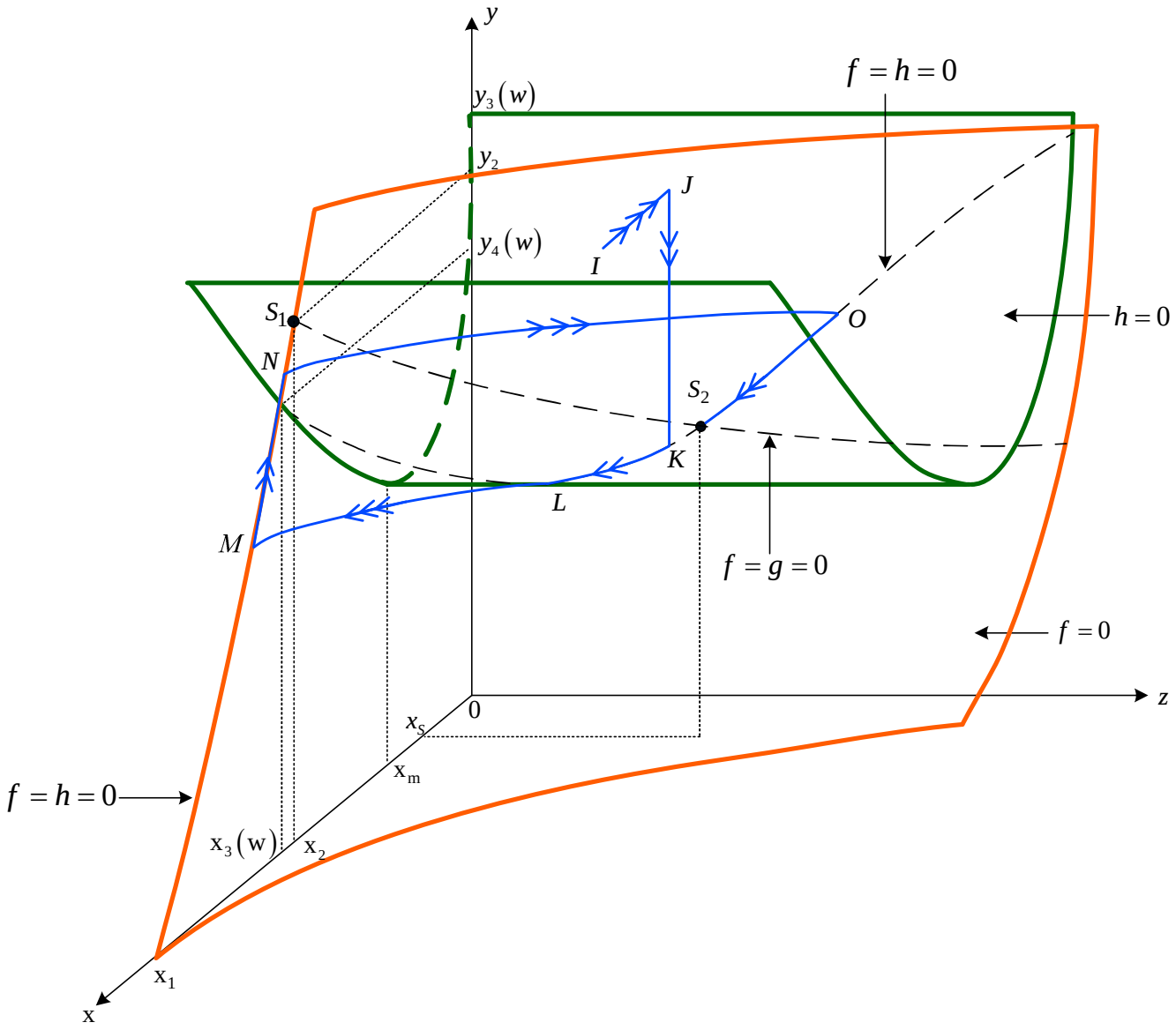

Fig. 3 The three equilibrium manifolds $\{f = 0\}, \{g = 0\}$ and $\{h = 0\}$ in the (x, y, z) – space in Case 3. Segments of the trajectories with one, two, and three arrows represent slow, fast, and very fast transitions, respectively.

IV. NUMERICAL RESULTS

A computer simulation of the system (5)-(8) with parametric values chosen to satisfy the condition in Case 1 is presented in Fig. 4. The solution trajectory, shown in Fig. 4a project onto the (x, y)-plane, tends to a limit cycle as theoretically predicted. The corresponding time courses of the concentration of PTH above the basal level, the level of serum vitamin D, the number of active osteoclasts and the number of active osteoblasts are as shown in Fig. 4b, 4c, 4d and 4e, respectively.

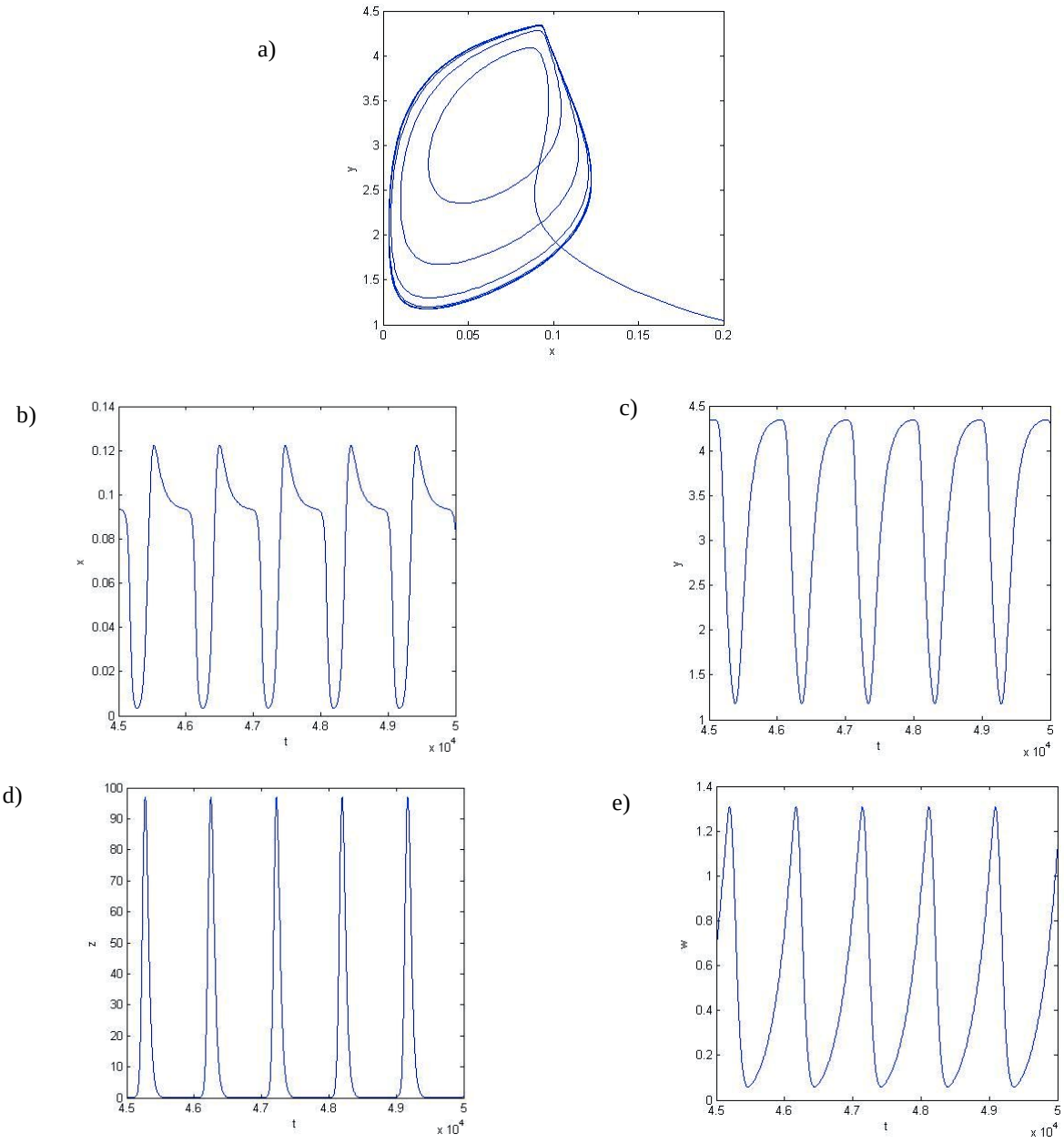

Fig. 4 A computer simulation of the model systems (5)-(8) with $c_1 = 0.1, c_2 = 0.8, c_3 = 0.8, c_4 = 0.5, c_5 = 0.1, c_6 = 0.1, c_7 = 0.1, c_8 = 0.95$, $k_1 = 1,\ k_2 = 2,\ k_3 = 5,\ k_4 = 3,\ k_5 = 1,\ k_6 = 5,\ d_1 = 0.1,\ d_2 = 0.04,\ d_3 = 0.3,\ d_4 = 0.4,\ \varepsilon = 0.2,\ \delta = 0.5,\ \eta = 0.9,\ x(0) = 0.5, y(0) = 0.2, z(0) = 1$ and $w(0) = 5$. (a) The solution trajectory projected onto the (*x*,*y*)-plane. (b) The corresponding time courses of the concentration of PTH above the basal level (*x*). (c) The corresponding time courses of the level of serum vitamin D (*y*), (d) number of active osteoclastic cells (*z*), and (e) number of active osteoblastic cells (*w*).

A computer simulation of the system (5)-(8) with parametric values chosen to satisfy the condition in Case 2 is presented in Fig. 5. The solution trajectory, shown in Fig. 5a project onto the (x, y)-plane, tends to a stable equilibrium as theoretically predicted. The corresponding time courses of the concentration of PTH above the basal level, the level of serum vitamin D, the number of active osteoclasts and the number of active osteoblasts are as shown in Fig. 5b, 5c, 5d and 5e, respectively

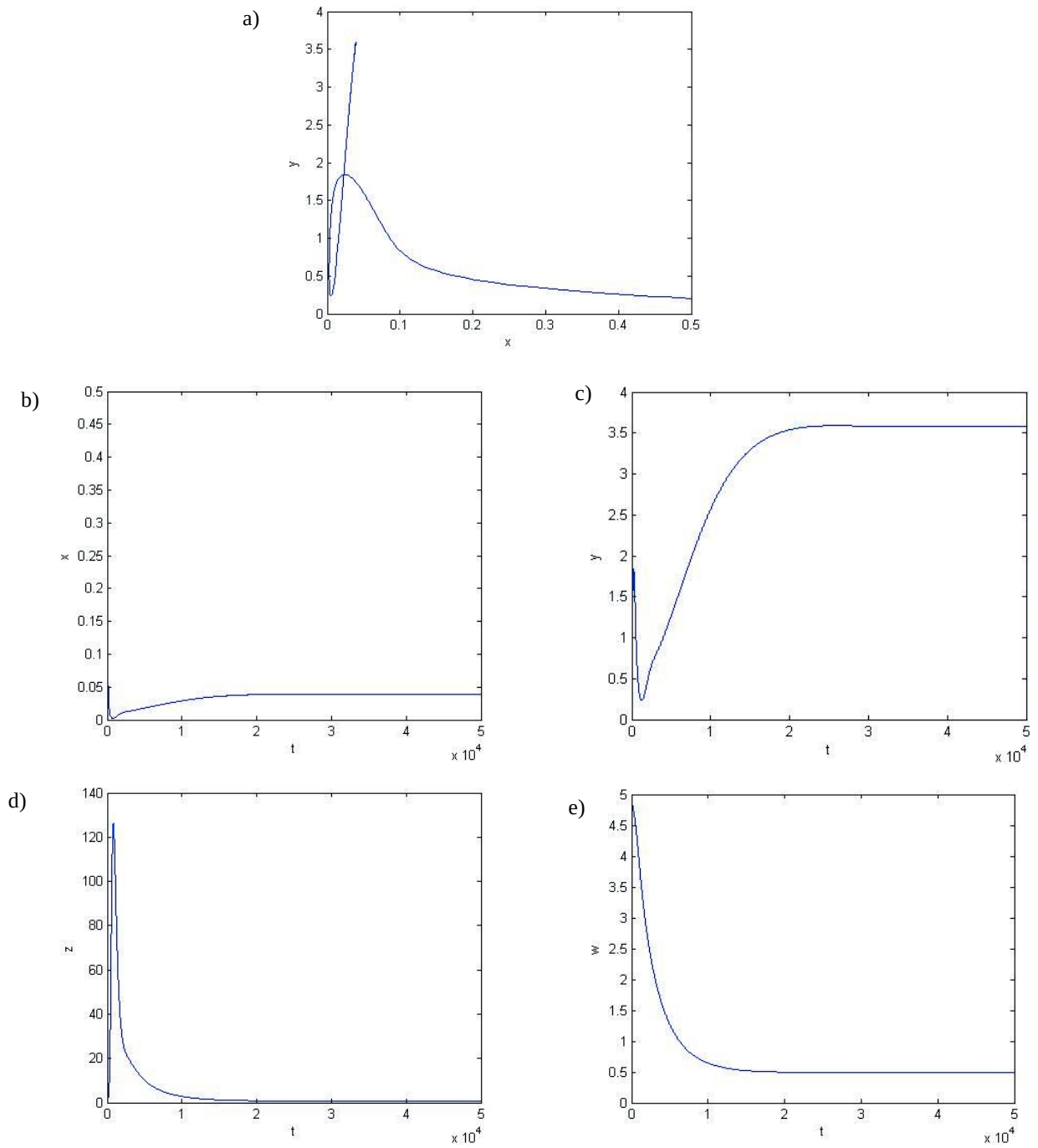

Fig. 5 A computer simulation of the model systems (5)-(8) with $c_1 = 0.05, c_2 = 0.8, c_3 = 0.8, c_4 = 0.5, c_5 = 0.1, c_6 = 0.1, c_7 = 0.1, c_8 = 0.95$, $k_1 = 1,\ k_2 = 2,\ k_3 = 5,\ k_4 = 3,\ k_5 = 1,\ k_6 = 5,\ d_1 = 0.1,\ d_2 = 0.04,\ d_3 = 0.3,\ d_4 = 0.4,\ \varepsilon = 0.1,\ \delta = 0.1,\ \eta = 0.1,\ x(0) = 0.5, y(0) = 0.2, z(0) = 1$ and $w(0) = 5$. (a) The solution trajectory projected onto the (*x*,*y*)-plane. (b) The corresponding time courses of the concentration of PTH above the basal level (*x*). (c) The corresponding time courses of the level of serum vitamin D (*y*), (d) number of active osteoclastic cells (*z*), and (e) number of active osteoblastic cells (*w*).

A computer simulation of the system (5)-(8) with parametric values chosen to satisfy the condition in Case 3 is presented in Fig. 6. The solution trajectory, shown in Fig. 6a project onto the (x, y)-plane, tends to a stable equilibrium as theoretically predicted. The corresponding time courses of the concentration of PTH above the basal level, the level of serum vitamin D, the number of active osteoclasts and the number of active osteoblasts are as shown in Fig. 6b, 6c, 6d and 6e, respectively

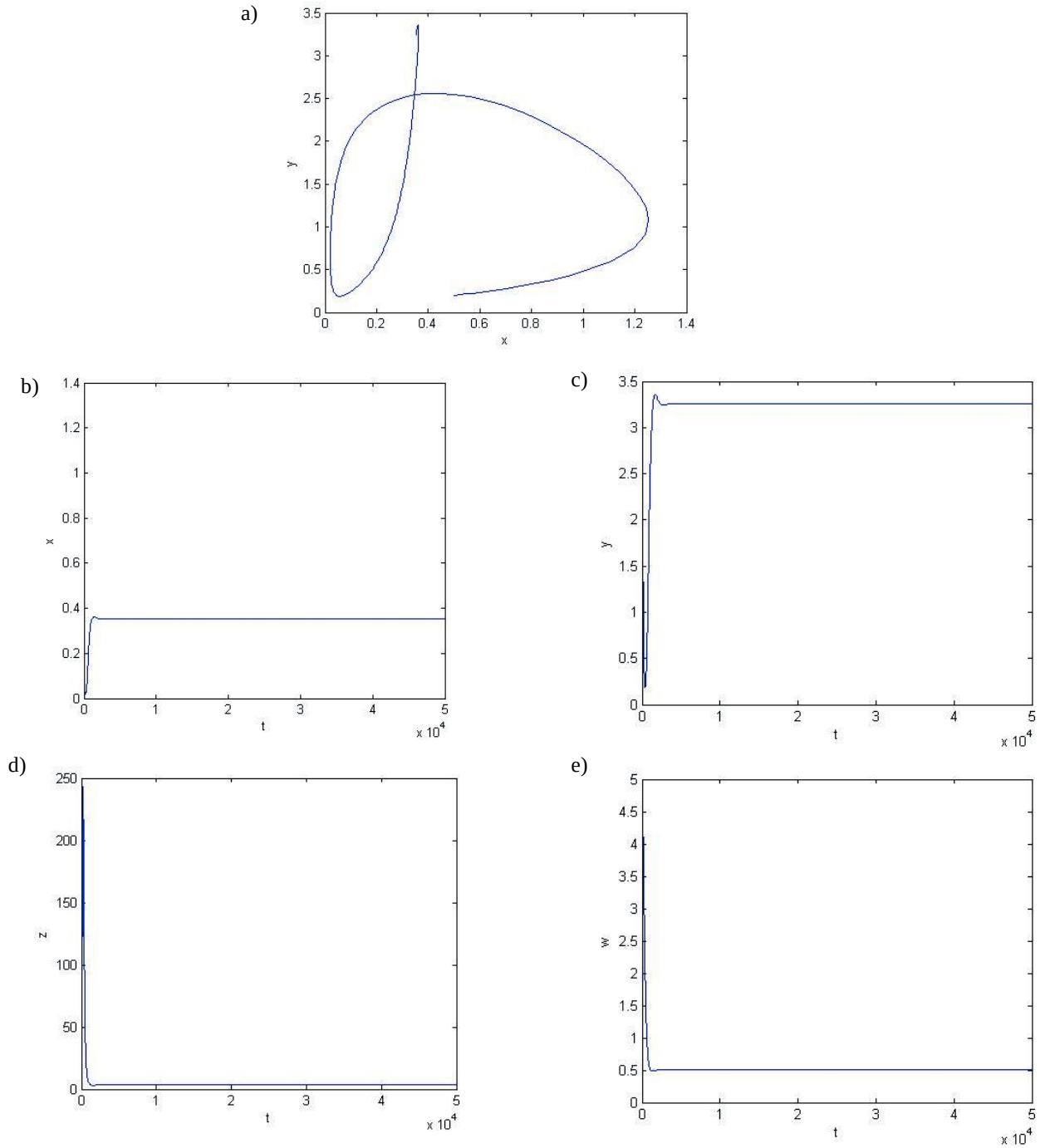

Fig. 6 A computer simulation of the model systems (5)-(8) with $c_1 = 0.8, c_2 = 0.8, c_3 = 0.8, c_4 = 0.5, c_5 = 0.2, c_6 = 0.1, c_7 = 0.1, c_8 = 0.95$, $k_1 = 1,\ k_2 = 2,\ k_3 = 5,\ k_4 = 3,\ k_5 = 1,\ k_6 = 5,\ d_1 = 0.1,\ d_2 = 0.04,\ d_3 = 0.3,\ d_4 = 0.4,\ \varepsilon = 0.3,\ \delta = 0.1,\ \eta = 0.3,\ x(0) = 0.5, y(0) = 0.2,$ $z(0) = 1$ and $w(0) = 5$. (a) The solution trajectory projected onto the (*x*,*y*)-plane. (b) The corresponding time courses of the concentration of PTH above the basal level (*x*). (c) The corresponding time courses of the level of serum vitamin D (*y*), (d) number of active osteoclastic cells (*z*), and (e) number of active osteoblastic cells (*w*).

V. CONCLUSION

In this paper, we developed a mathematical model to describe bone remodeling process by incorporating the effects of PTH and vitamin D on the proliferation and differentiation of osteoclastic and osteoblastic cells. We then apply the singular perturbation technique [15], [16] to our model in order to derive the conditions on the system parameters for which the various kinds of dynamic behavior can be obtained. We also investigated the model numerically by using Runge-Kutta method which has been widely used to find the approximate solution of the differential equations [17]-[20]. Theoretical and numerical results show that a periodic behavior can be exhibited by our model corresponding to the pulsatile secretion pattern of PTH and the oscillatory behavior observed clinically in the level of vitamin D [21]-[23].

REFERENCES

[1] H.M. Goodman, *Basic Medical Endocrinology*, 3rd edition, Academic Press, 2003.

[2] T. Russell, B. Turner, R. Lawrence, C.S. Thomas," Skeletal effects of estrogen", *Endocr. Rev.*, vol. 15, no. 3, pp.275-300, 1994.

[3] L.G. Raisz and B. E. Kream," Regulation of bone formation", *New Engl. J. Med.*, vol. 309, pp.29-35, 1983.

[4] E.M. Brown, "Extracellular Ca2+ sensing, regulation of parathyroid cell function, and role of Ca2+ and other ions as extracellular (first) messengers", *Physiol Rev*, vol. 71, pp. 371-411, 1991.

[5] M.F. Holick, "Vitamin D and Bone Health", *J. Nutr.*, vol. 126, pp. 1159S-1164S, 1996.

[6] H. Darwish and H.F. DeLuca, "Vitamin D-regulated gene expression", *Crit. Rev. Eukaryotic Gene Express*, Vol. 3, pp. 89-116, 1993.

[7] M.F. Holick, "Vitamin D: new horizons for the 21st century", Am. J. Clin. Nutr., vol. 60, pp. 619-630, 1994.

[8] M.F. Holick, "Vitamin D: photobiology, metabolism and clinical applications", in Endocrinology, 3rd edition, W.B. Saunders, Philadelphia, PA, 1995, pp. 990-1013.

[9] M.F. Holick, "Vitamin D and Bone Health", *J. Nutr.*, vol. 126, pp. 1159S-1164S, 1996.

[10] J.N.M. Heersche and S. Cherk, *Metabolic Bone Disease: cellular and tissue mechanisms*, Boca Raton, FI: CRC Press, 1989.

[11] A.W. Norman, G. Litwack, *Hormones*, 2nd edition, Academic Press, 1997.

[12] J.A. Albright and M. Sauders, *The Scientific Basis of Orthopaedics*, Norwalk, Conn: Appleton & Lange, 1990.

[13] M.H. Kroll, "Parathyroid hormone temporal effects on bone formation and resorption", *Bull. Math. Bio*, vol. 62, pp.163-188, 2000.

[14] H.V. Leeuwen, "Vitamin D and differentiation of mesenchymal stem cells and osteoblasts", *Endoc. Abs.*, vol. 22, pp. S14.4, 2010.

[15] T.J. Kaper, "An introduction to geometric methods and dynamical systems theory for singular perturbation problems. Analyzing multiscale phenomena using singular perturbation methods", *Proc. Symposia Appl Math*, vol. 56, 1999.

[16] S. Rinaldi and S. Muratori, "A separation condition for the existence of limit cycle in slow-fast systems", Appl Math Modelling, vol. 15, pp. 312-318, 1991.

[17] W. Sanprasert, U. Chundang and M. Podisuk, "Integration method and Runge-Kutta method", in *Proc. 15th American Conf. on Applied Mathematics*, WSEAS Press, Houston, USA, 2009, pp. 232.

[18] M. Racila and J.M. Crolet, "Sinupros: Mathematical model of human cortical bone", in *Proc. 10th WSEAS Inter. Conf. on Mathematics and Computers in Biology and Chemistry*, WSEAS Press, Prague, Czech Republic, 2009, pp. 53.

[19] N. Razali, R. R. Ahmed, M. Darus and A.S. Rambely, "Fifth-order mean Runge-Kutta methods applied to the Lorenz system", in *Proc. 13th WSEAS Inter. Conf. on Applied Mathematics*, WSEAS Press, Puerto De La Cruz, Tenerife, Spain, 2008, pp. 333.

[20] A. Chirita, R. H. Ene, R.B. Nicolescu and R.I. Carstea, "A numerical simulation of distributed-parameter systems", in *Proc. 9th WSEAS Inter. Conf. on Mathematic*al Methods and Computational Techniques in Electrical Engineering, WSEAS Press, Arcachon, 2007, pp. 70.

[21] K. N. Muse, S. C. Manolagas, L.J. Deftos, N. Alexander, and S.S.C. Yen, "Calcium-regulating hormones across the menstrual cycle", J. Clin. Endocrinol. Metab., vol.62, no.2, pp.1313-1315, 1986.

[22] V. Tangpricha, P. Koutkia, S.M. Rieke, T.C. Chen, A.A. Perez, and M.F. Holick, "Fortification of orange juice with vitamin D: a novel approach for enhancing vitamin D nutritional health", *Am. J. Clin. Nutr.*, vol. 77, pp. 1478-1483, 2003.

[23] M.F. Holick, "Sunlight and vitamin D for bone health and prevention of autoimmune diseases, cancers, and cardiovascular disease", *Am. J. Clin. Nutr.*, vol. 80 (suppl), pp. 1678S-1688S, 2004.